

Structure-Based Virtual Screening: An Application to Human Topoisomerase II α

Serge Christmann-Franck,^{†,‡} Hugues-Olivier Bertrand,[‡] Anne Goupil-Lamy,[‡] P. Arsène der Garabedian,[§] Olivier Mauffret,[†] Rémy Hoffmann,[‡] and Serge Fermandjian^{*,†}

Département de Biologie et Pharmacologie Structurales, UMR 8113 CNRS, LBPA, ENS Cachan, 61, avenue du Président Wilson, 94235 Cachan Cedex, France, Accelrys, 20, rue Jean Rostand, 91898 Orsay Cedex, France, and Laboratoire de Biochimie des Signaux Régulateurs Cellulaires et Moléculaires, Université Pierre et Marie Curie, CNRS FRE 2621, 96, Boulevard Raspail, 75006 Paris, France

Received April 1, 2004

The eukaryotic topoisomerase II is involved in several vital processes, such as replication, transcription, and recombination. Many compounds interfering with the catalytic action of this enzyme are efficient in human cancer chemotherapy. We applied a methodology combining molecular modeling and virtual screening techniques to identify human topoisomerase II α inhibitors. Data from structural biology and enzymatic assays together with a good background on the enzyme mechanism of action were helpful in the approach. A human topoisomerase II α model provided an insight into the structural features responsible for the activity of the enzyme. A protocol comprising several substructural and protein structure-based three-dimensional pharmacophore filters enabled the successful retrieving of inhibitors of the enzyme from large databases of compounds, thus validating the approach. A subset of protein structural features required for the enzyme inhibition at the protein–DNA interface were identified and incorporated into the pharmacophore models. Compounds sharing a DNA-intercalating chromophore and a moiety interfering with the protein active site emerged as good inhibitors.

Introduction

The identification of protein inhibitors can greatly benefit from the use of computer techniques. Among these, structure-based virtual screening requires pharmacophores designed from the protein three-dimensional structure.^{1,2} The use of pharmacophores allows the screening of large libraries of compounds and the retrieving of subsets of ligands displaying specific spatial arrangements of chemical features responsible for given types of activities.³ Development of new drugs for cancer therapy is highly necessary as such drugs often induce (multiple) drug resistance and must be increasingly renewed. Here, we focused on the human DNA topoisomerase II α as it represents a privileged primary target for many drugs currently used in cancer chemotherapy.^{4,5}

The infatuation for topoisomerases as possible drug targets started with the recognition of their critical role in cellular life. DNA topoisomerases I and II are ubiquitous enzymes that manage the topology of DNA during DNA replication, transcription, recombination, and chromatin remodeling.^{6–11} Topoisomerase I acts by passing one strand of the duplex through a break of the complementary strand,^{6,7} and topoisomerase II acts by passing a segment of duplex through a double-stranded break generated in the same or a different DNA.^{12,13} During the catalysis, a transient covalent complex is formed, usually referred to as cleavable complex, in which the enzyme is attached to the broken DNA. A

wide variety of molecules interfering with eukaryotic topoisomerase II activity have been recognized as potent anticancer drugs, many of them inducing cytotoxic lesions.^{4,14–17} They are often termed topoisomerase II inhibitors without distinguishing their mechanism of action, which can proceed according to two main routes: either by trapping the enzyme in the cleavable complex (topoisomerase II *poisons*), which in term leads to accumulation of truncated DNAs in the cell, therefore transforming the enzyme into a cellular poison,^{5,18} or by interfering with any other step of the catalytic cycle (topoisomerase II *catalytic inhibitors*) (for a recent review, see ref 19). Topoisomerase II poisons include DNA intercalators (anthracyclines such as FDA-approved doxorubicin, daunorubicin, and idarubicin;^{20–25} acridines²⁶ like bisantrene,^{27,28} actinomycins,²⁹ and ellipticines;^{30,31} anthracenediones such as mitoxantrone)³² and nonintercalators (epipodophyllotoxins such as VP-16 and VM-26^{33–36}) and also DNA minor-groove binders (distamycin, Hoechst33258,^{37,38} netropsin³⁹). Topoisomerase II catalytic inhibitors either interfere with binding of the enzyme to DNA (suramin,⁴⁰ aclarubicin⁴¹), stabilize noncovalent DNA-topoisomerase II complexes (merbarone,⁴² bisdioxopiperazines^{43,44}), or inhibit ATP binding (coumarines such as novobiocin⁴⁵).

Because an experimental structure of human topoisomerase II α was unavailable, we generated a model by homology modeling using the yeast topoisomerase II structure as a template. The so obtained model allowed a structure-based virtual screening to retrieve human topoisomerase II inhibitors interacting with critical active residues from databases. To our knowledge, no similar structure-based project targeting a eukaryotic topoisomerase has been reported thus far.

* To whom correspondence should be addressed. Tel +33 1 42 11 49 85. Fax: + 33 1 42 11 52 76. E-mail: sfermand@igr.fr.

[†] UMR 8113 CNRS.

[‡] Accelrys.

[§] Université Pierre et Marie Curie.



Figure 1. Model of the human topoisomerase II α dimer; the fold is similar to that of the experimental structures. Monomer 1 is depicted in light colors and monomer 2 in dark colors; A' subfragments are in blue, B' subfragments in green, HTH motifs in yellow, catalytic tyrosines in red, and active sites loops in brown. A DNA fragment (gray) was modeled in the DNA-binding domain of each monomer.

The only known structure-based drug design effort against a topoisomerase II concerns the DNA gyrase from *Escherichia coli*, which is a prokaryotic type II topoisomerase;⁴⁶ the work has proved successful in discovering a new inhibitor 10 times more potent than the drug novobiocin. Note also that Boehm and colleagues⁴⁶ have targeted the ATP binding site of the prokaryotic enzyme, while we have focused on a DNA-binding domain of the human protein.

Results and Discussion

Type II α topoisomerases are ubiquitous DNA-binding enzymes that catalyze the transport of one DNA double helix through another.^{6,7} Here we deal with the human DNA topoisomerase II α , for which no experimental structure has been reported yet. The three crystal structures presently available in the Protein Data Bank⁴⁷ concern the topoisomerase II core and DNA-binding domains of eukaryotic *Saccharomyces cerevisiae* (PDB accession numbers 1bgw⁴⁸ and 1bjt⁴⁹) and of prokaryotic *Escherichia coli* (PDB accession number 1ab4⁵⁰).

The eukaryotic topoisomerase II protein structures are homodimers. Each monomer is composed of an ATPase domain, of a A' subfragment bearing a DNA breakage/rejoining domain, and a B' subfragment, separated from the A' subfragment by a hinge⁴⁸) (Figure 1). The structure of the eukaryotic N terminal ATPase domain, connected to the B' subdomain, has been recently released (free protein, PDB accession number 1pvg;⁵¹ complex topoisomerase II-catalytic inhibitor Icrf-187, PDB accession number 1qzr⁵¹). The prokaryotic enzyme consists of two subunits, A and B, and the active form is an A₂B₂ tetramer. The A' and [B' + ATPase] parts of the eukaryotic enzyme are homologous to the

Table 1. Topoisomerases II from Several Organisms Used in the Multiple Sequences Alignment

entry name	accession no. ^a	organism
	1bgw (PDB)	<i>Saccharomyces cerevisiae</i>
	1bjt (PDB)	<i>Saccharomyces cerevisiae</i>
TOP2_YEAST	P06786 (SWP)	<i>Saccharomyces cerevisiae</i>
TOP2_BOMMO	O16140 (SWP)	<i>Bombyx mori</i>
TOP2_DROME	P15348 (SWP)	<i>Drosophila melanogaster</i>
TOP2_PEA	O24308 (SWP)	<i>Pisum sativum</i>
TOP2_PENCH	Q9Y8G8 (SWP)	<i>Penicillium chrysogenum</i>
TOP2_CRIFA	P2757 (SWP)	<i>Crithidia fasciculata</i>
TOP2_TRYCR	P30190 (SWP)	<i>Trypanosoma cruzi</i>
TOP2_ASFB7	Q00942 (SWP)	African swine fever virus (strain BA71V)
TP2A_HUMAN	P11388 (SWP)	<i>Homo sapiens</i>
TP2A_PIG	O46374 (SWP)	<i>Sus scrofa</i>
TP2A_MOUSE	Q01320 (SWP)	<i>Mus musculus</i>
TP2A_RAT	P41516 (SWP)	<i>Rattus norvegicus</i>
TP2A_CHICKEN	O42130 (SWP)	<i>Gallus gallus</i>
TP2B_HUMAN	Q02880 (SWP)	<i>Homo sapiens</i>
TP2B_MOUSE	Q64511 (SWP)	<i>Mus musculus</i>
TP2M_DICDI	P90520 (SWP)	<i>Dictyostelium discoideum</i>
O59854_ZYGRO	O59854 (SWP)	<i>Aspergillus nidulans</i>

^a The accession number is followed by the corresponding database, Swissprot (SWP) or Protein Databank (PDB).

prokaryotic A and B subunits, and the *E. coli* 1ab4 experimental structure exhibits a core and DNA binding domain (A subunit) equivalent to the *S. cerevisiae* A' subfragment.

The A' subfragment contains a "CAP-like" domain, so termed for its structural analogy to the DNA binding protein CAP (catabolic gene activator protein) of *E. coli* (CAP-DNA complex, PDB accession code 1cgp⁵²). The CAP-like domain includes a helix-turn-helix motif (HTH) (Figure 1) that has been recognized to contact DNA in a number of DNA-binding proteins⁵³ and that contains several strongly conserved residues. The catalytic tyrosine residue Y805, implicated in the cleavage of the phosphodiester DNA linkage (homologous to Y782 in *S. cerevisiae*⁵⁴), projects from a loop between the second and the third strand of the CAP-like domain, next to the helix $\alpha 4$ of the HTH motif (Figure 1). This loop is similar to the DNA backbone-contacting loop ("winged" motif) found in histone H5.⁵⁵ The current catalysis model suggests that each monomer of dimeric topoisomerase II binds one strand of the same double-stranded DNA and creates a transient break through the formation of a phosphotyrosine bond.^{48,56} According to this model, the DNA lays in a cleft between the A' and B' subfragments (Figure 1).

Template Selection and Preparation. The yeast topoisomerase II three-dimensional structure was used as a template for the homology modeling. The fact that this topoisomerase II presents a high sequence similarity with human topoisomerase II α (see thereafter) greatly facilitated the work. The A' subfragment that contains the DNA binding domain we wish to use for our compound identification has almost the same structure as in 1bgw and 1bjt (residues 683–1166; carbon α rmsd = 0.90 Å), while the 1bjt B' subfragment is rotated by nearly 170° from its position in the 1bgw structure.⁴⁹ Actually, 1bgw and 1bjt correspond to two distinct conformations adopted by the topoisomerase II molecule during the catalytic cycle. We intended to identify compounds interfering with the enzyme in the DNA-binding domain (located in the A' subfragment) and selected 1bgw as the template for homology modeling.

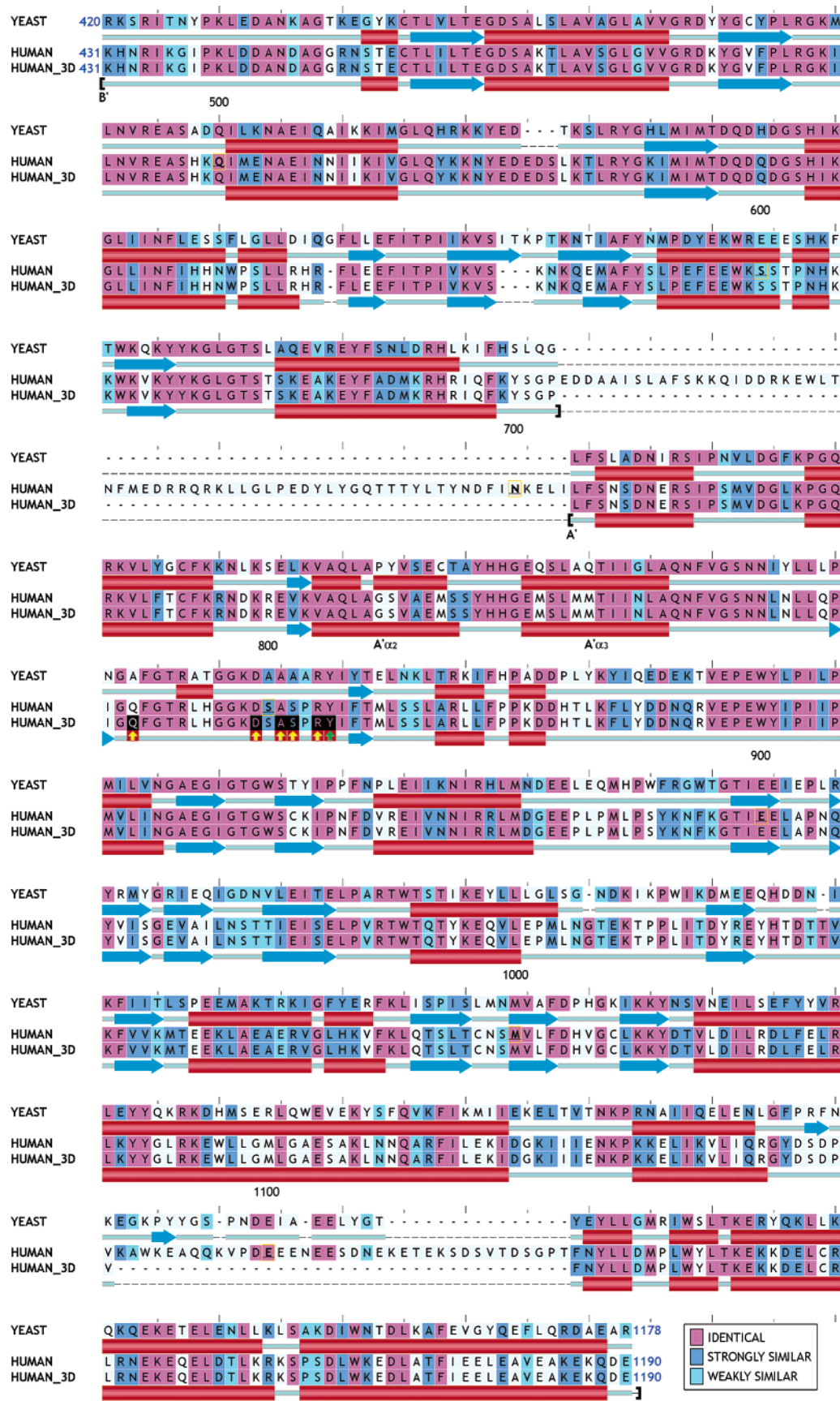


Figure 2. Sequence alignment used in comparative modeling, presenting the sequence of the yeast template structure 1bgw, the complete human sequence for the domain having a yeast structural equivalent, and the sequence of the three-dimensional human model. Identical residues are colored in mauve, strongly similar in dark blue, weakly similar in light blue, and nonmatching in light gray. The secondary structure elements are displayed below the sequences: helices are in red and sheets in blue. Arrows indicate the residues used to build the pharmacophore (yellow arrows), including the catalytic Y805 (green arrow). The A' and B' subfragments as well as helices $\alpha 3$ and $\alpha 4$ composing the HTH domain are labeled.

Table 2. Nature of the Selected Pharmacophoric Features^a

feature	residue	atom	feature	residue	atom
A1	R804	HH ₂₂	D2	Q789	OE ₁
A2	R804	HH ₂₁	D3	Y805	O
A3	R804/Y805	HH ₁₁ /HH	D4	D799	OD ₂
A4	S802	HN	L1	R804	CG
A5	R804/Y805	HH ₁₁ /HH	L2	Y805	benzene
A6	R804	HE	L3	A801	CB
D1	Y805	OH	L4	Y805	benzene

^a Pharmacophoric features run down the table and their corresponding structural elements run across the table (A, HBA, hydrogen-bond acceptor; D, HBD, hydrogen bond donor; L, LIPO, lipophilic interaction).

The dimer (biological unit of topoisomerase II α) of 1bgw was built from the monomer experimental structure. The resulting dimer was evaluated using Profiles_3D,^{57,58} this measuring the compatibility of an amino acid sequence with a three-dimensional protein structure. The dimer presented an acceptable Profiles_3D Overall Self-Compatibility Score equal to 95.8% of the maximum expected value for a protein of this size. No misfolded region was found in the area of the catalytic Y782 residue; 1.6% of the nonproline/glycine residues was located in a disallowed region of the Ramachandran map, none being located in the vicinity of Y782.

Sequence Alignment. The human DNA topoisomerase II α presents a closer sequence similarity to the eukaryotic *S. cerevisiae* protein than to the prokaryotic *E. coli* protein. To build a human DNA topoisomerase II α model, we generated an alignment of 19 sequences of DNA topoisomerase II (Table 1) which included the sequence of the template structure 1bgw (Figure 2). Human and *S. cerevisiae* DNA topoisomerase II sequences exhibited an identity of 47.3% and a similarity of 68.2%. This good sequence similarity, particularly at the DNA-binding domain, allowed the construction of a comparative model of reasonable quality for the human protein.

Comparative Modeling. On the basis of the 1bgw sequence alignment, a set of 10 three-dimensional models of dimeric human topoisomerase II α was constructed by comparative modeling. Dimeric templates were more appropriate than monomer templates for generating models taking into account the conformational changes occurring especially at the dimeriza-

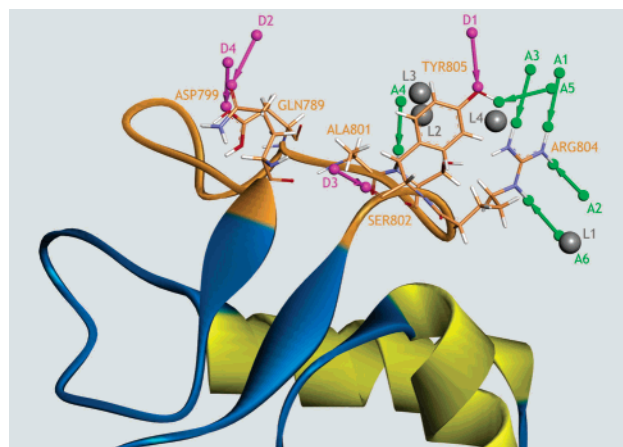


Figure 3. Graphical representation of the selected pharmacophoric features, superposed on the protein active site. HTH helices are shown in yellow, the active-site loop are in brown, and the pharmacophoric features are presented as arrows and spheres (A, HBA, hydrogen-bond acceptor, green arrows; D, HBD, hydrogen bond donor, purple arrows; L, LIPO, lipophilic interaction, gray spheres). The correspondence between features and enzyme chemical groups is detailed in Table 3.

tion interface. The overall quality of models was assessed using Modeler's PDF. The best model exhibited a satisfactory Profiles_3D Overall Self-Compatibility Score of 87.3% of the maximum expected value for a protein of this size. According to Modeler's PDF, no severe violations were observed. Only 1.2% of the residues of each monomer was located in a disallowed region of the Ramachandran map, and none was close to the catalytic Y805. The best model presents a similar profile to the template.

Definition of the Active Site. A cavity was detected just above the helix $\alpha 4$ of the HTH motif and close to the catalytic tyrosine Y805, located between the A' and B' subfragments. Amino acids belonging to the B' subfragment were not taken into account, to limit our search to inhibitors able to bind the A' domain, the conformation of which remains unchanged along the catalytic cycle.

Several residues that have been previously identified as being biologically important by site-directed mutagenesis experiments occupy this cavity. No substitu-

Table 3. Composition of the Pharmacophores^a

no. of features	pharmacophores																		
	1	2	3	4	5	6	7	8	9	10	11	12	13	14	15	16	17	18	19
A1	X	X	X	X	X	X	X	X	X	X				X	X		X	X	X
A2	X	X	X	X	X	X	X	X	X					X		X	X	X	X
A3	X	X	X					X		X									
A4											X	X	X						
A5				X										X	X	X		X	X
A6	X	X		X	X			X	X	X				X	X	X	X	X	X
D1	X		X	X		X		X	X		X		X	X	X	X	X		X
D2											X	X	X						
D3											X	X							
D4												X	X						
L1	X	X	X		X	X	X	X	X	X									
L2	X	X	X		X	X	X	X	X	X									
L3											X	X	X						
L4				X											X	X	X	X	X
Excl Vol	X	X	X	X	X	X	X	X	X	X	X	X	X	X	X	X	X	X	X

^a Pharmacophores run across the table and pharmacophoric features run down the table. A: HBA, hydrogen-bond acceptor. D: HBD, hydrogen-bond donor. L: LIPO, lipophilic interaction. Note: all pharmacophores include an identical set of 107 exclusion spheres.

Table 4. Screen of the NCI Database with the Three-Dimensional Pharmacophores: Distribution of the Hits^a

no. of features	pharmacophores												
	1	2	3	5	6	7	8	9	10	11	12	13	
total	0	0	0	5	1	21	41	62	189	3	14	20	
anticancer	0	0	0	1	1	0	11	14	27	1	6	2	
ratio	0	0	0	2.2	0.4	9.0	17.7	26.7	81.4	1.3	6.0	8.6	

^a For each pharmacophore are reported the numbers of pharmacophoric features, hits, known anticancer compounds among those hits, and the ratio of hits/database (in % $\times 10^2$).

tion of the catalytic Y805⁵⁹ was permitted, and only conservative substitutions were allowed at positions D799, A801, and R804.⁵⁹ A R781A mutant of yeast topoisomerase II (equivalent to a R804A mutant of human topoisomerase II) exhibited a nearly abolished activity.⁶⁰ D799, R804, and Y805 were conserved in all the sequences, and A801 in 17 of the 19 sequences was included in the alignment. They all belong to a loop at close distance from the DNA recognition helix $\alpha 4$ of the HTH motif. The loop contains also the solvent-accessible positively charged residues K798 and R804. Lysine and

Table 5. Structures of Some Topoisomerase II Inhibitors from the NCI Database Hit List and Pharmacophores that Identified the Hits

Name	Structure	Pharmacophore
valrubicin		10
detorubicin		10
aclarubicin		10
marcellomycin		10
piroxastrone		12
mithramycin		10
variamycin		6, 8, 9

Table 6. Anticancer Compounds from the NCI Database Hit List, with Some of Their Properties and Their Mechanism of Action

name, NCI code	details	activity, mechanism of action
valrubicin (NCI0246131)	non-DNA-binding ⁶⁷ derivative of the topoisomerase II targeting adriamycin anthracycline ⁶⁶	FDA approved for treatment of urinary bladder carcinoma ⁶⁸⁻⁷⁰
deterubicin (NCI0292652)	semisynthetic derivative of the topoisomerase II targeting daunorubicin anthracycline	active in clinical cancer therapy in non-Hodgkin lymphomas, carcinomas, soft-tissue sarcomas, melanoma ⁷¹⁻⁷⁴
aclarubicin (NCI0654508)	topoisomerase II targeting ⁷⁵ anthracycline isolated in 1975 from the culture of <i>Streptomyces galilaeus</i> MA144-M176	used in the treatment of acute lymphoid leukaemia ^{77,78}
marcellomycin (NCI0265211)	derivative of the topoisomerase II targeting aclarubicin anthracycline isolated from a bohemic acid complex ⁷⁹	antitumor properties, ⁷⁹ has been involved in several cancer therapy clinical trials ⁸⁰⁻⁸²
piroxastrone (NCI0349174)	first synthesized topoisomerase II-targeting anthrapyrazole	low activity against metastatic breast cancer in combination with high cardiac toxicity ⁸³
mithramycin (NCI0024559), variamycin (NCI0269146)	anticancer antibiotics ⁸⁴⁻⁸⁶ aureolic acids derivatives of chromomycin A3; ⁸⁸ chromomycin A3 inhibits prokaryotic ⁸⁹ and eukaryotic ⁹⁰ topoisomerase II catalytic activity	DNA minor groove binders ⁹¹⁻⁹³

arginine residues side-chains are known to interact electrostatically with DNA,⁶¹ which strengthens the active site localization hypothesis. Two other solvent-accessible residues of the loop (Q789, S802), specific to the mammalian topoisomerases II sequences as assessed by the Evolutionary Trace method, were finally included in the active site definition.

A study published after the completion of this project confirms the location of the active site and validates our selection of residues. It shows that T792, a loop residue close to the active site residues, is also involved in the enzyme catalysis.⁶²

The above-mentioned amino acid residues Q789, D799, A801, S802, R804, and Y805 were included in the active site definition. By targeting these residues, one can expect to identify compounds interfering with the enzyme activity by interacting either with the enzyme or with both the enzyme and the DNA at the DNA-protein interface. The interaction with DNA, if any, can occur either in the minor groove or between the bases through an intercalation mode. Note that pure DNA intercalators, that lack the chemical and structural groups necessary for binding to the enzyme, constitute a subtype of inhibitors (usually poisons) that are not identified during this search.

Pharmacophores, Virtual Screening. The pharmacophores based on the six selected residues were designed in a several step process (Table 2). These depict the features a ligand should possess to achieve a binding to the important active site residues of the enzyme. Interaction sites corresponding to the chemical nature of the residues were first built, and the 14 most representative structural features were converted into hydrophobic (LIPO), hydrogen-bond donor (HBD), and hydrogen-bond acceptor (HBA) pharmacophore features (Table 1, Table 3). Figure 3 displays those features in the protein active site.

Five-, six- and seven-feature pharmacophores were then built. Instead of building all the possible combinations using the 14 available features, which would have lead to a total of 8437 unique combinations, we manually designed 19 pharmacophores. LIPO features were present in the 19 pharmacophores. In 14 of them, a balance was kept between the HBA and HBD features, while the five remaining ones contained only HBA and LIPO features. The combinations of features were selected in such a way that they could cover the active site volume. A set of 107 exclusion spheres was finally

incorporated into each pharmacophore to sterically restrain the cavity allowed to the ligands.^{63,64} The pharmacophores were then used as filters to screen compound databases and identify the hits. As a hit is a molecule that maps all the features of its pharmacophore, the binding mode of each hit is defined by the interaction pattern of its pharmacophore. We started with the National Cancer Institute database⁶⁵ (NCI, 123 219 compounds), since this database gathers together compounds evaluated in anticancer projects.

A total of 318 unique compounds possessing chemical features matching the three-dimensional arrangement of the pharmacophoric features were retrieved with this first virtual screening. The hit distributions so obtained are presented in Table 4. The total number of hits over all pharmacophores exceeds 318, since some hits were identified by several pharmacophores. Note that the seven- and six-feature pharmacophores were too restrictive to identify a hit. In contrast, the five-feature pharmacophores allowed the identification of 35 anti-tumor topoisomerase II inhibitors or untested derivatives (as assessed by a bibliographic search based on their usual names when available and by visual inspection of their chemical structure) (Tables 4 and 5). Three major topoisomerase II inhibitor chemotypes were detected: anthracyclines (27 compounds), anthracenediones and anthrapyrazoles (six compounds), and aureolic acids (two compounds) (Table 6), all featuring a substituted planar conjugated ring system. The anthracyclines family included valrubicin and four adriamycin derivatives, deterubicin, aclarubicin (aclacinomycin A) and the related aclacinomycin X, 11-hydroxyaclacinomycin X, alcindoromycin, and marcellomycin, as well as three derivatives of daunomycin and three analogues of actinomycin (Table 5). The anthracenediones and anthrapyrazoles families have been developed in an effort to combine the broad antitumor activity of the anthracyclines with decreased myocardial toxicity.^{94,95} This chemotype included piroxastrone and several of its derivatives (Table 5). The two remaining compounds were the anticancer antibiotics aureolic acids mithramycin and variamycin,⁸⁸ derivatives of chromomycin A3 (Table 5). Chromomycin A3 is known to inhibit both the prokaryotic⁸⁹ and the eukaryotic⁹⁰ topoisomerase II catalytic activities.

Thus, our designed pharmacophores proved successful in retrieving known antitumor compounds. Although the intercalation property was not considered in our

Table 7. Structures of the Hits from the NCI Database Selected for DNA Relaxation Assay and the Pharmacophores that Identified the Hits

Name	Structure	Pharmacophore
NCI0007535		8
NCI0009223		11
NCI0107678		7, 12
NCI0245021		7, 10
NCI0402956		12
NCI0603831		10, 11
NCI0654508 aclarubicin		10
NCI0694885		7

pharmacophore construction, since no experimental structure of DNA–topoisomerase II complex is available

so far, most of the identified compounds exhibited DNA intercalator features (commonly a conjugated aromatic

Table 8. Screen of the Intercalating Subset of the WDI Database with the Three-Dimensional Pharmacophores: Distribution of the Hits^a

no. of features	pharmacophores																				
	1	2	3	4	5	6	7	8	9	10	11	12	13	14	15	16	17	18	19	20	21
total	0	0	0	72	314	179	397	77	77	203	144	167	204	257	192	151	168	443	557	398	782
anticancer	0	0	0	10	16	10	17	4	8	8	11	33	20	17	10	12	15	25	26	47	41
ratio	0	0	0	1.1	4.8	2.7	6.1	1.2	1.2	3.1	2.2	2.6	3.1	3.9	2.9	2.3	2.6	6.8	8.5	6.1	12.0

^a For each pharmacophore are reported the numbers of pharmacophoric features, hits, known anticancer compounds among those hits, and the ratio of hits/intercalating subset (in %).

ring system). Yet, two of the hits differ from the above ones: valrubicin is unable to intercalate into the intact double-stranded DNA but could insert its chromophore into the four nucleotide overhang of the topoisomerase II active site; aureolic acids bind DNA in the minor groove, where topoisomerases II are likely interacting with DNA. One can imagine a dual mechanism where the aureolic acids interact both with the enzyme active site and with the DNA at the cleavage site.

Another property shared by most of the identified compounds is their topoisomerase II poisoning activity. This is the case, for instance, for all the anthracyclines, except aclarubicin. The latter, although bearing the same structural features as the anthracyclines, acts as a catalytic inhibitor of topoisomerase II by preventing its binding to DNA.⁷⁵

The initial aim of this work was the search for new chemotypes of DNA topoisomerase II inhibitors displaying enzyme ligand properties. Seven compounds representative of the different chemotypes were selected from the complete NCI hit list to be tested in an experimental binding assay. None of these compounds bore an intercalating chromophore (shared by the known inhibitors of topoisomerase II of the hit list) and the anthracycline aclarubicin was added to the list (Table 7) to serve as a control for the enzyme inhibition by an inhibitor bearing a chromophore. Aclarubicin is interesting as it presents the double potential to intercalate into DNA through its chromophore, as proven by NMR experiments,⁹⁶ and to bind the enzyme through its three sugar groups, as suggested by virtual screening. The DNA relaxation results of the eight selected compounds revealed that aclarubicin was the only active compound, thus highlighting the importance of an intercalating chromophore to promote topoisomerase II inhibition. However, in contrast to the other known anthracyclines that are topoisomerase II poisons, aclarubicin is an inhibitor of the enzyme catalytic activity.⁷⁵

Globally, the virtual screening and experimental results conform to the common hypothesis that good topoisomerase II inhibitor candidates are compounds equipped with a planar aromatic ring system with a protruding side chain, where the ring system intercalates into the DNA base pairs while the side chain complements the binding by interacting either with the DNA or with the protein.^{97,98} Drugs working according to this model have one foot in the DNA and the other in the protein active site.⁹⁹ None of the here tested compounds lacking one of these two modes was found to be active. As shown with aclarubicin, upon its binding to the protein, the protruding side chain may block the catalytic activity, hindering the DNA cleavage.

We then designed a subset of compounds bearing a conjugated ring system and screened it with the topoi-

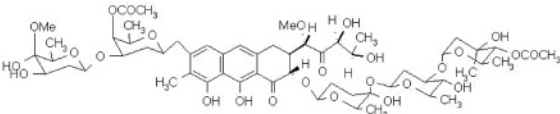
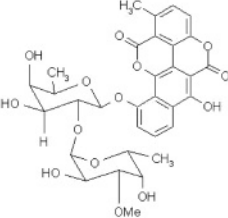
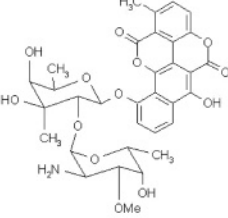
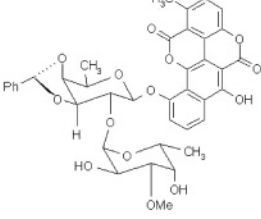
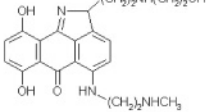
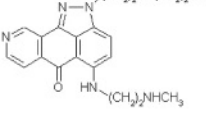
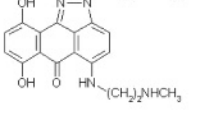
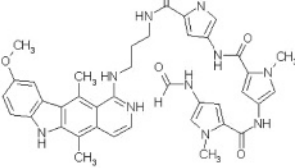
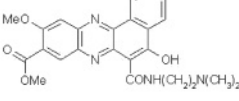
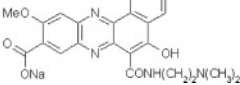
somerase II pharmacophores. With this focused screening, we expected to retrieve topoisomerase II inhibitors combining enzyme-binding and DNA intercalation features.

Two substructural pharmacophores representing the minimum features that a DNA intercalator should possess were therefore designed within the Catalyst program.¹⁰⁰ These pharmacophores were modified the naphthalene and indene scaffolds, mimicking minimal conjugated ring systems. They were used to prefilter the Derwent World Drug Index database (WDI, containing 53 964 marketed and development drugs¹⁰¹). A subset of 6536 compounds was so defined. Mining this subset of the database with the 19 previously designed topoisomerase II pharmacophores provided a second subset of 1255 different compounds (Table 8). As previously observed during the NCI screen, the seven-feature pharmacophores were too restrictive and failed to identify hits. The hits were composed of compounds having molecular weights up to 3000 and exhibiting up to 130 rotatable bonds. Large compounds shared a statistically increased ability to present three-dimensional arrangements of features resembling the pharmacophores. By reference to the properties of known topoisomerase II inhibitors, we discarded all the compounds having molecular weights larger than 1200, exhibiting more than 30 rotatable bonds, and inapt to intercalate into DNA according to visual inspection. This led to a final subset of 99 different compounds. Like the NCI hit list, this resulting WDI hit list gathers antitumor antibiotics and anthracenediones or anthrapyrazoles, this time totaling 60 (Table 8): seven angucyclines, 12 aureolic acids, chartreusin and six derivatives, 20 anthracenediones or anthrapyrazoles, and several other compounds. Among these, 27 are known topoisomerase II inhibitors. Table 9 presents the structures of compounds not already present in the NCI hit list and in Table 5, while Table 10 gives details about those compounds. The remaining compounds may also exhibit the topoisomerase II inhibition property, but this information is not available.

The WDI screening retrieved a majority of topoisomerase II poisons. All together, starting from a complete database, the use of a simple substructural filter significantly lowered the number of compounds to submit to the time-consuming three-dimensional pharmacophoric filtering. The enrichment was also noticeable as 27 of the 99 hits were known topoisomerase II inhibitors.

As observed in the NCI and WDI hit lists, a majority of identified topoisomerase II targeting compounds (i) bind the protein in the active site, as assessed by the location of the residues that the pharmacophores were designed from; (ii) exhibit a DNA intercalation ability;

Table 9. Structures of Some Topoisomerase II Inhibitors from the WDI Database Hit List

Name	Structure
chromomycin A3	
chartreusin	
elsamicin A	
A-132	
KW2170	
BBR-3438	
teloxantrone	
distel (1+)	
NC-182	
NC-190 ^(*)	

*NC-190 is not a hit but is presented as it is closely similar to NC-182.

Table 10. Anticancer Compounds from the WDI Database Hit List, with Some of Their Properties and Their Mechanism of Action

name	details	activity, mechanism of action
landomycin-A	angucycline antitumor antibiotic ^{103,104}	
urdamycin-D	angucycline antitumor antibiotic ¹⁰⁵	
gilvocarcin-E	angucycline antitumor antibiotic ¹⁰⁶	
chromomycin A3, mithramycin, variamycin, olivomycin chartreusin elsamicin A	anticancer antibiotics; ^{84–87} aureolic acid derivatives of chromomycin A3; ⁸⁸ chromomycin A3 inhibits prokaryotic ⁸⁹ and eukaryotic ⁹⁰ topoisomerase II catalytic activity	DNA minor groove binders ^{91–93}
A-132, IST-622	antitumor antibiotic topoisomerase II inhibitor, metabolite of the chartreusin derivative IST-622	shows activity against several tumor lines ¹⁰⁷ in phase II clinical trials in breast, colorectal, non-small-cell lung and ovarian cancer ^{109–111} phase II clinical trials in breast cancer ^{112–113}
piroxastrone,	topoisomerase II targeting anthracycline	low activity against metastatic breast cancer in combination with high cardiac toxicity ¹¹⁴
losoxastrone	topoisomerase II targeting anthracycline ¹¹⁵	high activity in the treatment of advanced breast cancer ^{116,117}
teloxastrone	topoisomerase II targeting anthracycline ¹¹⁵	in phase II clinical trials for metastatic malignant melanoma, non-small-cell lung cancer and colorectal carcinoma ^{118–120}
KW-2170 BBR-3438	topoisomerase II-targeting anthracycline ¹²¹ topoisomerase II-targeting anthracycline	entered phase II trials in 2001 for several cancers ^{121–123} demonstrated efficacy against human prostatic carcinoma, a tumor resistant to conventional antitumor drugs ¹²⁴
distel (1+)	dual topoisomerase I and II inhibitor, distamycinellipticine hybrid	DNA minor groove binder and intercalator ^{125,126}
NC-182	potent intercalator antitumor closely related to the antitumor topoisomerase II inhibitor NC-190 ¹²⁷	NC-190 was found to be active in several tumor lines ^{128,129}
citreamicin α	antitumor antibiotic ¹³¹	potent activity against a spectrum of Gram-positive aerobic and anaerobic bacteria ¹³⁰
elloramycin galtamycin clearmycin-A1 trioxacarcin-C	anthracycline-related antitumor antibiotic ^{132,133} antitumor antibiotic ¹³⁴ antitumor antibiotic ¹³⁵ antitumor antibiotic	active against stem cells of L-1210 leukemia ¹³² active against leukemia P388 and sarcoma 180 in mice ¹³⁵ found active in several tumor lines ¹³⁶

and (iii) act by poisoning the cleavable complex formed between topoisomerase II and DNA at the active site. In agreement with our findings, a recent article¹⁰² presents the docking of topoisomerase II inhibitors, including anthracycline derivatives, at the DNA cleavage site of a modeled topoisomerase II–cleaved DNA covalent complex. One can therefore imagine that the ensemble of pharmacophores globally depicts the different binding modes of poisons to the protein. No preference could be granted to a specific pharmacophore regarding its ability to depict a specific mechanism. For some compounds, the nature of the topoisomerase II inhibition mechanism (catalytic or by cleavable complex stabilization) was not reported in the literature. Aclarubicin was identified as a catalytic inhibitor blocking the access of the DNA to the active site residues. It seems to be the only nonpoison anthracycline, and a detailed study of its mechanism of inhibition will be the object of a future publication (unpublished results).

Conclusion

An approach by homology modeling and structure-based virtual screening using biochemistry and structural biology data enabled us to successfully determine several structural features that are the basis of human topoisomerase II inhibition at the DNA–protein interface. The inhibition results from a complex process that implicates several interacting molecules. Our analysis led to the proposal of a set of three-dimensional pharmacophores depicting the enzyme–drug interaction. The necessity of using a compound bearing an intercalating group to promote the enzyme inhibition appeared from the beginning of the work, so that the presence of this group was included in our screening protocol, as a

preliminary filter. One can wonder whether DNA intercalation is necessary for enzyme inhibition, per se, or whether it provides a way to conveniently anchor the drug in the active site. In the latter case, compounds anchored in the active site in the DNA minor groove and interacting with the active site residues could be efficient inhibitors. Our procedure could also be used to identify potential topoisomerase II α inhibitors in proprietary databases. The experimental resolution of a drug–DNA–enzyme complex could help to capture the fine structural details of the recognition event between topoisomerase II and its ligands. This would provide a guide for the search of more powerful anticancer drugs through a structure-based drug design process.

Experimental Section

Sequence Alignment. The human topoisomerase II α sequence (Swissprot Accession number P11388) was used as a query sequence to search the Swissprot and SP-TrEMBL databases using the BLASTp program.¹³⁷ Seventeen non-redundant sequences plus the sequences found in the *S. cerevisiae* DNA topoisomerase II crystal structures (PDB codes 1bgw⁴⁸ and 1bjt⁴⁹) were selected (Table 1). The sequences were aligned using CLUSTALW.¹³⁸ The alignment was then manually refined in order to avoid gaps in the secondary structure elements (Figure 2). Two insertions having no structural equivalent were discarded (E644-L705, 63 residues; K1088-T1124, 38 residues) (Figure 2).

Comparative Modeling. The template crystal structure of *S. cerevisiae* topoisomerase II α (PDB code 1bgw, residues E409–D1201) was built as a dimer using symmetry operations deduced of the transformation matrix available in the PDB file. A set of 10 three-dimensional dimeric models of the human protein was then constructed by comparative modeling, including residues K431–E1190 in each monomer (Figure 2). The models were generated using Modeler 6.00.⁵⁷ The overall

quality of the models was assessed using Modeler's Probability Density Functions (PDF), Profiles_3D,⁵⁸ and Ramachandran maps.

Active-Site Definition. The active site was defined using a combination of convergent methods. Cavities were detected using a flood-filling algorithm. This was achieved in mapping the protein to a grid. The grid points at a certain distance from the protein atoms were labeled as occupied by the protein; the cavity was then defined from the set of all unoccupied grid points. An "eraser" algorithm was used to clean all grid points outside the protein, and a flood-filling algorithm was employed to search unoccupied, connected grid points, which form the cavities. The evolutionary trace method was applied to define important binding residues (binding site analysis method^{57,139,140}). This method is based on the extraction of functionally important residues from sequence-conservation patterns in homologous proteins and on their mapping onto the protein surface to generate clusters identifying functional interfaces. We also identified from the site-directed mutagenesis literature the residues important for the enzyme activity.^{59,60} A visual inspection of the identified residues location within the active site helped us select six residues (Q789, D799, A801, S802, R804, and Y805) that were subsequently used to define the pharmacophores.

Structure-Based Pharmacophores Design. Structure-based pharmacophores were designed using the structure-based focusing method.¹⁴¹ The program generates a Ludi interaction map^{142,143} describing all the possible interactions (hydrogen-bond donors and acceptors, hydrophobic) that a ligand can establish with a given active site. A map was generated for all atoms within a radius of 12 Å of the active site center, defined as the geometric center of the six selected residues. The pharmacophoric features corresponding to the six residues were clustered, and 14 features were finally selected. They consisted of six hydrogen-bond donors (HBA, able to create a hydrogen bond with the protein through their hydrogen), four hydrogen-bond acceptors (HBD, able to create a hydrogen bond with a hydrogen of the protein), and four hydrophobic groups (LIPO) (detailed in Results and Discussion). Table 1 presents the list of pharmacophoric features and identifies the protein atoms they were generated from and the corresponding residues. Groups of five to seven features out of 14 were then combined to design 19 pharmacophores. The combinations were designed to ensure active site volume coverage while including pharmacophoric features belonging to different types, focusing rather on representativity of the pharmacophores than on their exhaustivity. An identical set of 107 exclusion spheres (radius = 1.2 Å) was included in each pharmacophore, to mimic the noninteracting protein atoms that the ligand is not allowed to penetrate and to limit the size of the allowed cavity.^{63,64} A sphere of 7 Å radius was defined, centered on the geometric center of the selected amino acids. Exclusion volume spheres were placed on each heavy atom of the protein found in this sphere, using a 1.2 Å radius. Some exclusion volume spheres were then manually removed in Catalyst to simplify the pharmacophores. Table 3 details the composition of each pharmacophore in terms of pharmacophoric features.

Database Virtual Screening. The Catalyst-formatted database of the National Cancer Institute⁶⁵ (NCI, version 2000, 123 219 compounds) was screened with the generated pharmacophores as three-dimensional queries using Catalyst's catSearch.¹⁰⁰ Each compound is stored in the databases with a collection of conformations that represent the conformational diversity within a given conformational energy range (20 kcal/mol by default). For each conformation, the geometrical fit between the chemical features and the features of all pharmacophores was assessed. A hit is a compound that maps all pharmacophoric features, which excludes partial mappings. A set of diverse compounds was manually selected and submitted to a DNA relaxation assay to assess the quality of the pharmacophores.

The experimental results led us to the conclusion that an intercalating scaffold was necessary for the activity of the

compounds. Therefore, the Derwent World Drug Index¹⁰¹ (WDI, version 1999, 53 964 compounds) was first filtered using two simple substructural pharmacophores (modified naphthalene and indene scaffolds, in which atoms were substituted or nonsubstituted carbon or nitrogen atoms, all substitutions being allowed) to retrieve potential DNA intercalators. Appropriate compounds (MW lower than 1200, number of rotatable bonds lower than 30) were then screened with the structure-based designed pharmacophores.

Topoisomerase II Relaxation Assay. Relaxation experiments were performed with a supercoiled pBR322 DNA and human topoisomerase II α from TopoGen. The reaction mixture contained 10 mM Tris-HCl (pH 8.0), 100 mM KCl, 8 mM MgCl₂, 0.5 mM DTT, 10 mM ATP, and 2% glycerol. The drugs (0.005–300 μ M) were incubated for 5 min at 0–4 °C with 0.25 unit topoisomerase II before adding 0.05 μ g of pBR322 DNA. The reaction was allowed to proceed for 2.5 min at 37 °C. The enzymatic reaction was then stopped by addition of ¹/₁₀ volume 4% SDS, 0.3% bromophenol blue, 50% sucrose. The electrophoretic analysis was performed in 1.2% agarose slab gels (11.5 × 13.5 × 0.5 cm) in an electrophoresis buffer containing 36 mM Tris base/1 mM EDTA/30 mM sodium phosphate. Current was applied at 50 V for 4 h for relaxation, with recirculation of buffer between reservoirs. Following electrophoresis, gels were stained for 15 min in ethidium bromide at 2 mg/mL in bidistilled water and transferred into bidistilled water for another 15 min. Gels were then illuminated from below with a shortwave ultraviolet light plate and photographs were taken with a digital camera.

Note that 1 unit of human topoisomerase II can relax 0.02 μ g of pBR322 in 1 min at 37 °C.

Acknowledgment. This work was supported by a CIFRE grant from Accelrys and the French Ministry of Research (S.C.F.). The authors wish to acknowledge the excellent assistance of Jon Sutter for the virtual screening experiments.

References

- (1) Kubinyi, H. Structure-based design of enzyme inhibitors and receptors ligands. *Curr. Opin. Drug. Discovery Dev.* **1998**, *1*, 4–15.
- (2) Babine, R. E.; Bender, S. L. Molecular Recognition of Protein–Ligand Complexes: Applications to Drug Design. *Chem. Rev.* **1997**, *97*, 1359–1472.
- (3) Hoffren, A. M.; Murray, C. M.; Hoffmann, R. D. Structure-based focusing using pharmacophores derived from the active site of 17 β -hydroxysteroid dehydrogenase. *Curr. Pharm. Des.* **2001**, *7*, 547–566.
- (4) Chen, A. Y.; Liu, L. F. DNA topoisomerases: Essential enzymes and lethal targets. *Annu. Rev. Pharmacol. Toxicol.* **1994**, *34*, 191–218.
- (5) Froelich-Ammon, S. J.; Osheroff, N. Topoisomerase poisons: Harnessing the dark side of enzyme mechanism. *J. Biol. Chem.* **1995**, *270*, 21429–21432.
- (6) Gellert, M. DNA topoisomerases. *Annu. Rev. Biochem.* **1981**, *50*, 879–910.
- (7) Wang, J. C. DNA topoisomerases. *Annu. Rev. Biochem.* **1985**, *54*, 665–697.
- (8) Vosberg, H. P. DNA topoisomerases: Enzymes that control DNA conformation. *Curr. Top. Microbiol. Immunol.* **1985**, *114*, 9–102.
- (9) Cozzarelli, N. R.; Wang, J. C. *DNA topology and its biological effects*; Cold Spring Harbor Laboratory Press: Cold Spring Harbor, NY, 1990.
- (10) Wang, J. C.; DNA topoisomerases. *Annu. Rev. Biochem.* **1996**, *65*, 635–692.
- (11) Champoux, J. J.; DNA topoisomerases: Structure, function, and mechanism. *Annu. Rev. Biochem.* **2001**, *70*, 369–413.
- (12) Osheroff, N.; Zechiedrich, E. L.; Gale, K. C. Catalytic function of DNA topoisomerase II. *Bioessays* **1991**, *13*, 269–273.
- (13) Berger, J. M. Type II DNA topoisomerases. *Curr. Opin. Struct. Biol.* **1998**, *8*, 26–32.
- (14) Capranico, G.; Zunino, F. DNA topoisomerase-trapping antitumour drugs. *Eur. J. Cancer* **1992**, *28A*, 2055–2060.
- (15) Liu, L. DNA Topoisomerases: Topoisomerase-targeted drugs. In *Advances in Pharmacology*; Academic Press: New York, 1994; Vol. 29.

- (16) Sinha, B. K. Topoisomerase inhibitors. A review of their therapeutic potential in cancer. *Drugs* **1995**, *49*, 11–19.
- (17) Malonne, H.; Atassi, G. DNA topoisomerase targeting drugs: Mechanisms of action and perspectives. *Anticancer Drugs* **1997**, *8*, 811–822.
- (18) Corbett, A. H.; Osheroff, N. When good enzymes go bad: Conversion of topoisomerase II to a cellular toxin by antineoplastic drugs. *Chem. Res. Toxicol.* **1993**, *6*, 585–597.
- (19) Larsen, A. K.; Escargueil, A. E.; Skladanowski, A. Catalytic topoisomerase II inhibitors in cancer therapy. *Pharmacol. Ther.* **2003**, *99*, 167–181.
- (20) Arcamone, F.; Cassinelli, G.; Fantini, G.; Grein, A.; Orezzi, P.; Pol, C.; Spalla, C. Adriamycin, 14-hydroxydaunomycin, a new antitumor antibiotic from *S. peucetius* var. *caesius*. *Biotechnol. Bioeng.* **1969**, *11*, 1101–1110.
- (21) Di Marco, A.; Casazza, A. M.; Gambetta, R.; Supino, R.; Zunino, F. Relationship between activity and amino sugar stereochemistry of daunorubicin and adriamycin derivatives. *Cancer Res.* **1976**, *36*, 1962–1966.
- (22) Zunino, F.; Gambetta, R.; DiMarco, A.; Luoni, G.; Zaccara, A. Effects of the stereochemical configuration on the interaction of some daunomycin derivatives with DNA. *Biochem. Biophys. Res. Commun.* **1976**, *69*, 744–750.
- (23) Tewey, K. M.; Rowe, T. C.; Yang, L.; Halligan, B. D.; Liu, L. F. Adriamycin-induced DNA damage mediated by mammalian DNA topoisomerase II. *Science* **1984**, *226*, 466–468.
- (24) Berman, E. A review of idarubicin in acute leukemia. *Oncology (Huntington)* **1993**, *7*, 91–98, 104; discussion 104–107.
- (25) Feig, S. A.; Ames, M. M.; Sather, H. N.; Steinherz, L.; Reid, J. M.; Trigg, M.; Pendergrass, T. W.; Warkentin, P.; Gerber, M.; Leonard, M.; Bleyer, W. A.; Harris, R. E. Comparison of idarubicin to daunomycin in a randomized multidrug treatment of childhood acute lymphoblastic leukemia at first bone marrow relapse: A report from the Children's Cancer Group. *Med. Pediatr. Oncol.* **1996**, *27*, 505–514.
- (26) Rowe, T. C.; Chen, G. L.; Hsiang, Y. H.; Liu, L. F. DNA damage by antitumor acridines mediated by mammalian DNA topoisomerase II. *Cancer Res.* **1986**, *46*, 2021–2026 (27) Yap, H. Y.; Yapn, B. S.; Blumenschein, G. R.; Barnes, B. C.; Schell, F. C.; Bodey, G. P. Bisantrene, an active new drug in the treatment of metastatic breast cancer. *Cancer Res.* **1983**, *43*, 1402–1404.
- (27) Yap, H. Y.; Yapn, B. S.; Blumenschein, G. R.; Barnes, B. C.; Schell, F. C.; Bodey, G. P. Bisantrene, an active new drug in the treatment of metastatic breast cancer. *Cancer Res.* **1983**, *43*, 1402–1404.
- (28) Coltman, C. A., Jr; Osborne, C. K. Bisantrene, biological and clinical effects. *Cancer Treat. Rev.* **1984**, *11*, 285–288.
- (29) Woodruff, H. B.; Waksman, S. A. The actinomycins and their importance in the treatment of tumors in animals and man. Historical background. *Ann. NY Acad. Sci.* **1960**, *89*, 287–298.
- (30) Ross, W. E.; Bradley, M. O. DNA double-stranded breaks in mammalian cells after exposure to intercalating agents. *Biochim. Biophys. Acta* **1981**, *654*, 129–134.
- (31) Tewey, K. M.; Chen, G. L.; Nelson, E. M.; Liu, L. F. Intercalative antitumor drugs interfere with the breakage-reunion reaction of mammalian DNA topoisomerase II. *J. Biol. Chem.* **1984**, *259*, 9182–9187.
- (32) Crespi, M. D.; Ivanier, S. E.; Genovese, J.; Baldi, A. Mitoxantrone affects topoisomerase activities in human breast cancer cells. *Biochem. Biophys. Res. Commun.* **1986**, *136*, 521–528.
- (33) Chen, G. L.; Yang, L.; Rowe, T. C.; Halligan, B. D.; Tewey, K. M.; Liu, L. F. Nonintercalative antitumor drugs interfere with the breakage-reunion reaction of mammalian DNA topoisomerase II. *J. Biol. Chem.* **1984**, *259*, 13560–13566.
- (34) Ross, W.; Rowe, T.; Glisson, B.; Yalowich, J.; Liu, L. Role of topoisomerase II in mediating epipodophyllotoxin-induced DNA cleavage. *Cancer Res.* **1984**, *44*, 5857–5860.
- (35) Long, B. H.; Musial, S. T.; Brattain, M. G. Comparison of cytotoxicity and DNA breakage activity of congeners of podophyllotoxin including VP16–213 and VM26: A quantitative structure–activity relationship. *Biochemistry* **1984**, *23*, 1183–1188.
- (36) Long, B. H.; Musial, S. T.; Brattain, M. G. Single- and double-strand DNA breakage and repair in human lung adenocarcinoma cells exposed to etoposide and teniposide. *Cancer Res.* **1985**, *45*, 3106–3112.
- (37) Fesen, M.; Pommier, Y. Mammalian topoisomerase II activity is modulated by the DNA minor groove binder distamycin in simian virus 40 DNA. *J. Biol. Chem.* **1989**, *264*, 11354–11359.
- (38) Woynarowski, J. M.; McHugh, M.; Sigmund, R. D.; Beerman, T. A. Modulation of topoisomerase II catalytic activity by DNA minor groove binding agents distamycin, Hoechst 33258, and 4',6-diamidino-2-phenylindole. *Mol. Pharmacol.* **1989**, *35*, 177–182.
- (39) Beerman, T. A.; Woynarowski, J. M.; Sigmund, R. D.; Gawron, L. S.; Rao, K. E.; Lown, J. W. Netropsin and bis-netropsin analogues as inhibitors of the catalytic activity of mammalian DNA topoisomerase II and topoisomerase cleavable complexes. *Biochim. Biophys. Acta* **1991**, *1090*, 52–60.
- (40) Bojanowski, K.; Lelievre, S.; Markovits, J.; Couprie, J.; Jacquemin-Sablon, A.; Larsen, A. K. Suramin is an inhibitor of DNA topoisomerase II in vitro and in Chinese hamster fibrosarcoma cells. *Proc. Natl. Acad. Sci. U.S.A.* **1992**, *89*, 3025–3029.
- (41) Sorensen, B. S.; Sinding, J.; Andersen, A. H.; Alsnér, J.; Jensen, P. B.; Westergaard, O. Mode of action of topoisomerase II-targeting agents at a specific DNA sequence. Uncoupling the DNA binding, cleavage and religation events. *J. Mol. Biol.* **1992**, *228*, 778–786.
- (42) Drake, F. H.; Hofmann, G. A.; Mong, S. M.; Bartus, J. O.; Hertzberg, R. P.; Johnson, R. K.; Mattern, M. R.; Mirabelli, C. K. In vitro and intracellular inhibition of topoisomerase II by the antitumor agent merbarone. *Cancer Res.* **1989**, *49*, 2578–2583.
- (43) Ishida, R.; Miki, T.; Narita, T.; Yui, R.; Sato, M.; Utsumi, K. R.; Tanabe, K.; Andoh, T. Inhibition of intracellular topoisomerase II by antitumor bis(2,6-dioxopiperazine) derivatives: Mode of cell growth inhibition distinct from that of cleavable complex-forming type inhibitors. *Cancer Res.* **1991**, *51*, 4909–4916.
- (44) Tanabe, K.; Ikegami, Y.; Ishida, R.; Andoh, T. Inhibition of topoisomerase II by antitumor agents bis(2,6-dioxopiperazine) derivatives. *Cancer Res.* **1991**, *51*, 4903–4908.
- (45) Gormley, N. A.; Orphanides, G.; Meyer, A.; Cullis, P. M.; Maxwell, A. The interaction of coumarin antibiotics with fragments of DNA gyrase B protein. *Biochemistry* **1996**, *35*, 5083–5092.
- (46) Boehm, H. J.; Boehringer, M.; Bur, D.; Gmuender, H.; Huber, W.; Klaus, W.; Kostrewa, D.; Kuehne, H.; Luebbers, T.; Meunier-Keller, N.; Mueller, F.; Novel inhibitors of DNA gyrase: 3D structure based biased needle screening, hit validation by biophysical methods, and 3D guided optimization. A promising alternative to random screening. *J. Med. Chem.* **2000**, *43*, 2664–2674.
- (47) Berman, H. M.; Westbrook, J.; Feng, Z.; Gilliland, G.; Bhat, T. N.; Weissig, H.; Shindyalov, I. N.; Bourne, P. E. The Protein Data Bank. *Nucleic Acids Res.* **2000**, *28*, 235–242.
- (48) Berger, J. M.; Gamblin, S. J.; Harrison, S. C.; Wang, J. C. Structure and mechanism of DNA topoisomerase II. *Nature* **1996**, *379*, 225–232.
- (49) Fass, D.; Bogden, C. E.; Berger, J. M. Quaternary changes in topoisomerase II may direct orthogonal movement of two DNA strands. *Nat. Struct. Biol.* **1999**, *16*, 322–326.
- (50) Morais Cabral, J. H.; Jackson, A. P.; Smith, C. V.; Shikotra, N.; Maxwell, A.; Liddington, R. C. Crystal structure of the breakage-reunion domain of DNA gyrase. *Nature* **1997**, *388*, 903–906.
- (51) Classen, S.; Olland, S.; Berger, J. M. Structure of the topoisomerase II ATPase region and its mechanism of inhibition by the chemotherapeutic agent ICRF-187. *Proc. Natl. Acad. Sci. U.S.A.* **2003**, *100*, 10629–10634.
- (52) Schultz, S. C.; Shields, G. C.; Steitz, T. A. Crystal structure of a CAP-DNA complex: The DNA is bent by 90 degrees. *Science* **1991**, *253*, 1001–1007.
- (53) Harrison, S. C.; Aggarwal, A. K. DNA recognition by proteins with the helix–turn–helix motif. *Annu. Rev. Biochem.* **1990**, *59*, 933–969.
- (54) Worland, S. T.; Wang, J. C. Inducible overexpression, purification, and active site mapping of DNA topoisomerase II from the yeast *Saccharomyces cerevisiae*. *J. Biol. Chem.* **1989**, *264*, 4412–4416.
- (55) Ramakrishnan, V.; Finch, J. T.; Graziano, V.; Lee, P. L.; Sweet, R. M. Crystal structure of globular domain of histone H5 and its implications for nucleosome binding. *Nature* **1993**, *362*, 219–223.
- (56) Roca, J.; Wang, J. C. The capture of a DNA double helix by an ATP-dependent protein clamp: A key step in DNA transport by type II DNA topoisomerases. *Cell* **1992**, *71*, 833–840.
- (57) Insight-II 2000, Accelrys Inc., San Diego, CA.
- (58) Fischer, D.; Eloffson, A.; Rice, D.; Eisenberg, D. Assessing the performance of fold recognition methods by means of a comprehensive benchmark. *Pac. Symp. Biocomput.* **1996**, 300–318 (59) Okada, Y.; Ito, Y.; Kikuchi, A.; Nimura, Y.; Yoshida, S.; Suzuki, M. Assignment of functional amino acids around the active site of human DNA topoisomerase II alpha. *J. Biol. Chem.* **2000**, *275*, 24630–24638.
- (59) Liu, Q.; Wang, J. C. Identification of active site residues in the “GyrA” half of yeast DNA topoisomerase II. *J. Biol. Chem.* **1998**, *273*, 20252–20256.
- (60) Nadassy, K.; Wodak, S. J.; Janin, J. Structural features of protein–nucleic acid recognition sites. *Biochemistry* **1999**, *38*, 1999–2017.
- (61) Suda, N.; Nakagawa, Y.; Kikuchi, A.; Sawada, M.; Takami, Y.; Funahashi, H. O.; Nakao, A.; Yoshida, S.; Suzuki, M. Function of the loop residue Thr792 in human DNA topoisomerase II alpha. *Biochem. Biophys. Res. Commun.* **2003**, *28*, 46–51.

- (62) Greenidge, P. A.; Carlsson, B.; Bladh, L. G.; Gillner, M. Pharmacophores incorporating numerous excluded volumes defined by X-ray crystallographic structure in three-dimensional database searching: Application to the thyroid hormone receptor. *J. Med. Chem.* **1998**, *41*, 2503–2512.
- (63) Gillner, M.; Greenidge, P. The use of multiple excluded volumes derived from X-ray crystallographic structures in 3D database searching and 3D QSAR. In *Pharmacophore Perception, Development, and Use in Drug Design*; Güner, O. F., Ed., Int. University Line: La Jolla, CA, 2000; pp 371–384.
- (64) http://www.accelrys.com/catalyst/cat_dbs.html; <http://ntp.nci.nih.gov/>
- (65) Israel, M.; Modest, E. J.; Frei, E., III. *N*-Trifluoroacetyl Adriamycin-14-valerate, an analogue with greater experimental antitumor activity and less toxicity than adriamycin. *Cancer Res.* **1975**, *35*, 1365–1368.
- (66) Israel, M.; Potti, G. Adriamycin analogues. Preparation and biological evaluation of some *N*-perfluoroacyl analogues of daunorubicin, adriamycin, and *N*-(trifluoroacetyl)adriamycin 14-valerate and their 9,10-anhydro derivatives. *J. Med. Chem.* **1982**, *25*, 187–191.
- (67) Blum, R. H.; Garnick, M. B.; Israel, M.; Pannelos, G. P.; Henderson, I. C.; Frei, E., III. Preclinical rationale and phase I clinical trial of the adriamycin analogue, AD 32. *Recent Results Cancer Res.* **1981**, *41*, 7–15.
- (68) Niell, H. B.; Hunter, R. F.; Herrod, H. G.; Israel, M. Effects of *N*-trifluoroacetyl adriamycin-14-valerate (AD-32) on human bladder tumor cell lines. *Cancer Chemother. Pharmacol.* **1987**, *19*, 47–52.
- (69) Kuznetsov, D. D.; Alsikafi, N. F.; O'Connor, R. C.; Steinberg, G. D. Intravesical valrubicin in the treatment of carcinoma in situ of the bladder. *Expert. Opin. Pharmacother.* **2001**, *2*, 1009–1013.
- (70) Maral, R.; Heusse, D.; Lavelle, F.; Cueille, G.; Marlard, M.; Jacquillat, C.; Maral, J.; Auclerc, M. F.; Weil, M.; Auclerc, G.; Bernard, J. Experimental and clinical activity of a new anthracycline derivative: Detorubicin (14-diethoxyacetoxidaunorubicin). *Recent Results Cancer Res.* **1980**, *40*, 172–183.
- (71) No authors listed. Clinical study of detorubicin. EORTC Clinical Screening Group. *Recent Results Cancer Res.* **1980**, *40*, 184–191.
- (72) Chawla, S. P.; Legha, S. S.; Benjamin, R. S. Detorubicin—An active anthracycline in untreated metastatic melanoma. *J. Clin. Oncol.* **1985**, *3*, 1529–1534.
- (73) Colbert, N.; Vannetzel, J. M.; Izrael, V.; Schlienger, M.; Milleron, B.; Blanchon, F.; Herman, D.; Akoun, G.; Roland, J.; Chatelet, F. A prospective study of detorubicin in malignant mesothelioma. *Cancer* **1985**, *56*, 2170–2174.
- (74) Jensen, P. B.; Sorensen, B. S.; Demant, E. J.; Sehested, M.; Jensen, P. S.; Vindelov, L.; Hansen, H. H. Antagonistic effect of aclarubicin on the cytotoxicity of etoposide and 4'-(9-acridinylamino)methanesulfon-*m*-anisidide in human small cell lung cancer cell lines and on topoisomerase II-mediated DNA cleavage. *Cancer Res.* **1990**, *50*, 3311–3316.
- (75) Oki, T.; Matsuzawa, Y.; Yoshimoto, A.; Numata, K.; Kitamura, I.; Hori, S.; Takamatsu, A.; Umezawa, H.; Ishizuka, M.; Nagawana, H.; Suda, H.; Hamada, M.; Takeuchi, T. New antitumor antibiotics aclacinomycin A and B. *J. Antibiot. (Tokyo)* **1975**, *28*, 830–834.
- (76) Suzuki, H.; Kawashima, K.; Yamada, K. Aclacinomycin A, a new anti-leukaemic agent. *Lancet* **1979**, *1*, 870–871.
- (77) Oki, T.; Takeuchi, T.; Oka, S.; Umezawa, H. New anthracycline antibiotic aclacinomycin A: Experimental studies and correlations with clinical trials. *Recent Results Cancer Res.* **1981**, *41*, 21–40.
- (78) Nettleton, D. E. Jr; Bradner, W. T.; Bush, J. A.; Coon, A. B.; Moseley, J. E.; Myllymaki, R. W.; O'Herron, F. A.; Schreiber, R. H.; Vulcano, A. L. New antitumor antibiotics: Musettamycin and marcellomycin from bohemian acid complex. *J. Antibiot. (Tokyo)* **1977**, *30*, 525–529.
- (79) Nicaise, C.; Rozenzweig, M.; de Marneffe, M.; Crespeigne, N.; Dodium, P.; Piccart, M.; Sculier, J. P.; Lenaz, J.; Kenis, Y. Clinical phase I trial of marcellomycin with a single-dose schedule. *Eur. J. Cancer Clin. Oncol.* **1983**, *19*, 449–454.
- (80) Joss, R. A.; Kaplan, S.; Goldhirsch, A.; Varini, M.; Brunner, K. W.; Cavalli, F. A phase I trial of marcellomycin with a weekly dose schedule. *Eur. J. Cancer Clin. Oncol.* **1983**, *19*, 455–459.
- (81) Wadler, S.; Fuks, J. Z.; Wiernik, P. H. Phase I and II agents in cancer therapy: I. Anthracyclines and related compounds. *J. Clin. Pharmacol.* **1986**, *26*, 491–509.
- (82) Ingle, J. N.; Kuross, S. A.; Mailliard, J. A.; Loprinzi, C. L.; Jung, S. H.; Nelimark, R. A.; Krook, J. E.; Long, H. J. Evaluation of piroxantrone in women with metastatic breast cancer and failure on nonanthracycline chemotherapy. *Cancer* **1994**, *74*, 1733–1738.
- (83) Terent'eva, T. G.; Sokolov, A. B.; Navashin, S. M. Comparative experimental antitumor activity of the antibiotics variamycin and mitramycin. *Antibiotiki* **1978**, *23*, 349–351.
- (84) Radzievskaia, V. V.; Terent'eva, T. G.; Sokolov, A. B. Action of aureolic acid and dactinomycin group antibiotics on human brain tumors in culture. *Antibiotiki* **1978**, *23*, 103–109.
- (85) Singh, B.; Gupta, R. S. Species-specific differences in the toxicity and mutagenicity of the anticancer drugs mithramycin, chromomycin A3, and olivomycin. *Cancer Res.* **1985**, *45*, 2813–2820.
- (86) Kuru, M. Clinical experience with a new antitumor agent chromomycin. *Cancer Chemother. Rep.* **1961**, *13*, 91–97.
- (87) Slavik, M.; Carter, S. K. Chromomycin A3, mithramycin, and olivomycin: Antitumor antibiotics of related structure. *Adv. Pharmacol. Chemother.* **1975**, *12*, 1–30.
- (88) Simon, H.; Wittig, B.; Zimmer, C. Effect of netropsin, distamycin A and chromomycin A3 on the binding and cleavage reaction of DNA gyrase. *FEBS Lett.* **1994**, *353*, 79–83.
- (89) Bell, A.; Kittler, L.; Lober, G.; Zimmer, C. Influence of minor groove binders on the eukaryotic topoisomerase II cleavage reaction with 41 base pair model oligonucleotides. *Invest. New Drugs* **1996**, *13*, 271–84.
- (90) Baguley, B. C. Nonintercalative DNA-binding antitumor compounds. *Mol. Cell. Biochem.* **1982**, *43*, 167–181.
- (91) Banville, D. L.; Keniry, M. A.; Shafer, R. H. NMR investigation of mithramycin A binding to d(ATGCAT)₂: A comparative study with chromomycin A3. *Biochemistry* **1990**, *29*, 9294–9304.
- (92) Sastry, M.; Patel, D. J. Solution structure of the mithramycin dimer-DNA complex. *Biochemistry* **1993**, *32*, 6588–6604.
- (93) Showalter, H. D.; Johnson, J. L.; Hoftiezer, J. M.; Turner, W. R.; Werbel, L. M.; Leopold, W. R.; Shillis, J. L.; Jackson, R. C.; Elslager, E. F. Anthrapyrazole anticancer agents. Synthesis and structure-activity relationships against murine leukemias. *J. Med. Chem.* **1987**, *30*, 121–131.
- (94) Judson, I. R. Anthrapyrazoles: True successors to the anthracyclines? *Anti-Cancer Drugs* **1991**, *2*, 223–231.
- (95) Yang, D.; Wang, A. H. Structure by NMR of antitumor drugs aclacinomycin A and B complexed to d(CGTCAG). *Biochemistry* **1994**, *33*, 6595–6604.
- (96) Macdonald, T. L.; Lehnert, E. K.; Loper, J. T.; Chow, K.-C.; Ross, W. E. In *DNA Topoisomerases in Cancer*; Potmesil, M.; Kohn, K. W., Eds.; Oxford University Press: New York, 1991, 199–214.
- (97) Capranico, G.; Binaschi, M. DNA sequence selectivity of topoisomerases and topoisomerase poisons. *Biochim. Biophys. Acta* **1998**, *1400*, 185–194.
- (98) Huff, A. C.; Kreuzer, K. N. Evidence for a common mechanism of action for antitumor and antibacterial agents that inhibit type II DNA topoisomerases. *J. Biol. Chem.* **1990**, *265*, 20496–20505.
- (99) Catalyst4.8, Accelrys Inc., San Diego, CA.
- (100) http://www.accelrys.com/catalyst/cat_dbs.html; <http://www.derwent.com/products/lr/wdi/>
- (101) Moro, S.; Beretta, G.L.; Dal Ben, D.; Nitiss, J.; Palumbo, M.; Capranico, G.
- (102) Interaction model for anthracycline activity against DNA topoisomerase II. *Biochemistry* **2004**, *43*, 7503–13.
- (103) Henkel, T.; Rohr, J.; Beale, J. M.; Schwenen, L. Landomycins, new angucycline antibiotics from *Streptomyces* sp. I. Structural studies on landomycins A–D. *J. Antibiot. (Tokyo)* **1990**, *43*, 492–503.
- (104) Crow, R. T.; Rosenbaum, B.; Smith, R., III; Guo, Y.; Ramos, K. S.; Sulikowski, G. A. Landomycin A inhibits DNA synthesis and G1/S cell cycle progression. *Bioorg. Med. Chem. Lett.* **1999**, *9*, 1663–1666.
- (105) Rohr, J.; Zeeck, A.; Floss, H. G. Urdamycins, new angucycline antibiotics from *Streptomyces fradiae*. III. The structures of urdamycins C and D. *J. Antibiot. (Tokyo)* **1988**, *41*, 126–129.
- (106) Balitz, D. M.; O'Herron, F. A.; Bush, J.; Vyas, D. M.; Nettleton, D. E.; Grulich, R. E.; Bradner, W. T.; Doyle, T. W.; Arnold, E.; Clardy, J. Antitumor agents from *Streptomyces anandii*: Gilvocarins V, M and E. *J. Antibiot. (Tokyo)* **1981**, *34*, 1544–1555.
- (107) McGovern, J. P.; Neil, G. L.; Crampton, S. L.; Robinson, M. I.; Dourous, J. D. Antitumor activity and preliminary drug disposition studies on chartreusin (NSC5159). *Cancer Res.* **1977**, *37*, 1666–1672.
- (108) Loricco, A.; Long, B. H.; Biochemical characterisation of elsamicin and other coumarin-related antitumor agents as potent inhibitors of human topoisomerase II. *Eur. J. Cancer* **1993**, *29A*, 1985–1991.
- (109) Verweij, J.; Wanders, J.; Nielsen, A. L.; Pavlidis, N.; Calabresi, F.; ten Bokkel Huinink, W.; Brunsch, U.; Piccart, M.; Franklin, H.; Kaye, S. B. Phase II studies of Elsamicin in breast cancer, colorectal cancer, nonsmall cell lung cancer and ovarian cancer. EORTC Early Clinical Trials Group. *Ann. Oncol.* **1994**, *5*, 375–376.
- (110) Konishi, M.; Sugawara, K.; Kofu, F.; Nishiyama, Y.; Tomita, K.; Miyaki, T.; Kawaguchi, H. Elsamicins, new antitumor antibiotics related to chartreusin. I. Production, isolation, characterization and antitumor activity. *J. Antibiot. (Tokyo)* **1986**, *39*, 784–791.
- (111) Silvestrini, R.; Sanfilippo, O.; Zaffaroni, N.; De Marco, C.; Catania, S.; Activity of a chartreusin analogue, elsamicin A, on breast cancer cells. *Anticancer Drugs* **1992**, *3*, 677–681.

- (112) Tashiro, T.; Kon, K.; Yamamoto, M.; Yamada, N.; Tsuruo, T.; Tsukagoshi, S. Antitumor effects of IST-622, a novel synthetic derivative of chartreusin, against murine and human tumor lines following oral administration. *Cancer Chemother. Pharmacol.* **1994**, *34*, 287–292.
- (113) Asai, G.; Yamamoto, N.; Toi, M.; Shin, E.; Nishiyama, K.; Sekine, T.; Nomura, Y.; Takashima, S.; Kimura, M.; Tominaga, T. Pharmacokinetic and pharmacodynamic study of IST-622, a novel synthetic derivative of chartreusin, by oral administration in a phase II study of patients with breast cancer. *Cancer Chemother. Pharmacol.* **2002**, *49*, 468–472.
- (114) Ingle, J. N.; Kuross, S. A.; Mailliard, J. A.; Loprinzi, C. L.; Jung, S. H.; Nelimark, R. A.; Krook, J. E.; Long, H. J. Evaluation of piroxantrone in women with metastatic breast cancer and failure on nonanthracycline chemotherapy. *Cancer* **1994**, *74*, 1733–1738.
- (115) Leteurtre, F.; Kohlhagen, G.; Paull, K. D.; Pommier, Y. Topoisomerase II inhibition and cytotoxicity of the anthrapyrazoles DuP 937 and DuP 941 (Losoaxantrone) in the National Cancer Institute preclinical antitumor drug discovery screen. *J. Natl. Cancer Inst.* **1994**, *86*, 1239–1244.
- (116) Talbot, D. C.; Smith, I. E.; Mansi, J. L.; Judson, I.; Calvert, A. H.; Ashley, S. E. Anthrapyrazole CI941: A highly active new agent in the treatment of advanced breast cancer. *J. Clin. Oncol.* **1991**, *9*, 2141–2147.
- (117) Vandenberg, T. A. New developments in chemotherapy for metastatic breast cancer. *Anticancer Drugs* **1994**, *5*, 251–259.
- (118) Shore, T.; Eisenhauer, E.; Quirt, I.; Belanger, K.; Lohmann, R.; Silver, H.; Wielgosz, G. A phase II study of DuP 937 (Teloxantrone) in metastatic malignant melanoma: A study of the National Cancer Institute of Canada Clinical Trials Group (NCICCTG). *Ann. Oncol.* **1993**, *4*, 695–696.
- (119) Gregg, R. W.; Kaizer, L.; Fine, S.; Gelmon, K.; Wielgosz, G.; Eisenhauer, E. A phase II trial of DuP 937 (Teloxantrone) in nonsmall cell lung cancer. A study of the NCIC Clinical Trials Group. *Ann. Oncol.* **1993**, *4*, 693–694.
- (120) Maroun, J. A.; Skillings, J.; MacCormick, R.; Potvin, M.; Wielgosz, G.; Davidson, J. R.; Eisenhauer, E. Phase II study on DuP 937 (Teloxantrone) in colorectal carcinoma. A Canadian National Cancer Institute Clinical Trial Group study. *Invest. New Drugs* **1993**, *11*, 235–237.
- (121) Verschraegen, C. F. KW-2170 (Kyowa Hakko Kogyo). *IDrugs*. **2002**, *5*, 1000–1003.
- (122) Sugaya, T.; Mimura, Y.; Shida, Y.; Osawa, Y.; Matsukuma, I.; Ikeda, S.; Akinaga, S.; Morimoto, M.; Ashizawa, T.; Okabe, M. 6H-Pyrazolo[4,5,1-de]acridin-6-ones as a novel class of antitumor agents. Synthesis and biological activity. *J. Med. Chem.* **1994**, *37*, 1028–1032.
- (123) Ashizawa, T.; Shimizu, M.; Gomi, K.; Okabe, M. Antitumor activity of KW-2170, a novel pyrazoloacridone derivative. *Anticancer Drugs* **1998**, *9*, 263–271.
- (124) Supino, R.; Polizzi, D.; Pavesi, R.; Pratesi, G.; Guano, F.; Capranico, G.; Palumbo, M.; Sissi, C.; Richter, S.; Beggiolin, G.; Menta, E.; Pezzoni, G.; Spinelli, S.; Torriani, D.; Carenini, N.; Dal Bo, L.; Facchinetti, F.; Tortoreto, M.; Zunino, F. A novel 9-aza-anthrapyrazole effective against human prostatic carcinoma xenografts. *Oncology* **2001**, *61*, 234–242.
- (125) Bailly, C.; Leclere, V.; Pommery, N.; Colson, P.; Houssier, C.; Rivalle, C.; Bisagni, E.; Henichart, J. P. Binding to DNA, cellular uptake and biological activity of a distamycin–ellipticine hybrid molecule. *Anticancer Drug Des.* **1993**, *8*, 145–164.
- (126) Riou, J. F.; Grondard, L.; Naudin, A.; Bailly, C. Effects of two distamycin–ellipticine hybrid molecules on topoisomerase I and II mediated DNA cleavage: Relation to cytotoxicity. *Biochem. Pharmacol.* **1995**, *50*, 424–428.
- (127) Yamagishi, T.; Nakaike, S.; Ikeda, T.; Ikeya, H.; Otomo, S. A novel antitumor compound, NC-190, induces topoisomerase II-dependent DNA cleavage and DNA fragmentation. *Cancer Chemother. Pharmacol.* **1996**, *38*, 29–34.
- (128) Tarui, M.; Doi, M.; Ishida, T.; Inoue, M.; Nakaike, S.; Kitamura, K. DNA-binding characterization of a novel anti-tumour benzo[a]phenazine derivative NC-182: Spectroscopic and viscometric studies. *Biochem. J.* **1994**, *304*, 271–279.
- (129) Nakaike, S.; Yamagishi, T.; Samata, K.; Nishida, K.; Inazuki, K.; Ichihara, T.; Migita, Y.; Otomo, S.; Aihara, H.; Tsukagoshi, S. In vivo activity on murine tumors of a novel antitumor compound, N-beta-dimethylaminoethyl 9-carboxy-5-hydroxy-10-methoxybenzo[a]phenazine-6-carboxamide sodium salt (NC-190). *Cancer Chemother. Pharmacol.* **1989**, *23*, 135–139.
- (130) Maiese, W. M.; Lechevalier, M. P.; Lechevalier, H. A.; Korshalla, J.; Goodman, J.; Wildey, M. J.; Kuck, N.; Greenstein, M. LL-E19085 alpha, a novel antibiotic from *Micromonospora citrea*: Taxonomy, fermentation and biological activity. *J. Antibiot (Tokyo)* **1989**, *42*, 846–851.
- (131) Carter, G. T.; Nietsche, J. A.; Williams, D. R.; Borders, D. B. Citreamicins, novel antibiotics from *Micromonospora citrea*: Isolation, characterization, and structure determination. *J. Antibiot (Tokyo)*. **1990**, *43*, 504–512.
- (132) Drautz, H.; Reuschenbach, P.; Zahner, H.; Rohr, J.; Zeeck, A. Metabolic products of microorganisms. 225. Elloramycin, a new anthracycline-like antibiotic from *Streptomyces olivaceus*. Isolation, characterization, structure and biological properties. *J. Antibiot (Tokyo)* **1985**, *38*, 1291–1301.
- (133) Fiedler, H. P.; Rohr, J.; Zeeck, A. Elloramycins B, C, D, E and F: minor congeners of the elloramycin producer *Streptomyces olivaceus*. *J. Antibiot (Tokyo)* **1986**, *39*, 856–859.
- (134) Korobkova, T. P.; Singal, E. M.; Ivanitskaia, L. P.; Kudina, M. K.; Karbyshev, V. D. The antibiotic galtamycin. Its fermentation, isolation, physicochemical and biological properties. *Antibiot. Med. Biotekhnol.* **1986**, *31*, 428–431.
- (135) Fujii, N.; Katsuyama, T.; Kobayashi, E.; Hara, M.; Nakano, H. The clearmycins, new antitumor antibiotics produced by *Streptomyces*: Fermentation, isolation and biological properties. *J. Antibiot (Tokyo)* **1995**, *48*, 768–772.
- (136) Fujimoto, K.; Morimoto, M. Antitumor activity of trioxacarcin C. *J. Antibiot (Tokyo)*. **1983**, *36*, 1216–1221.
- (137) Altschul, S. F.; Madden, T. L.; Schaffer, A. A.; Zhang, J.; Zhang, Z.; Miller, W.; Lipman, D. J. Gapped BLAST and PSI-BLAST: A new generation of protein database search programs. *Nucleic Acids Res.* **1997**, *25*, 3389–3402.
- (138) Thompson, J. D.; Higgins, D. G.; Gibson, T. J. CLUSTAL W: Improving the sensitivity of progressive multiple sequence alignment through sequence weighting, position-specific gap penalties and weight matrix choice. *Nucleic Acids Res.* **1994**, *22*, 4673–4680.
- (139) Lichtarge, O.; Bourne, H. R.; Cohen, F. E. An evolutionary trace method defines binding surfaces common to protein families. *J. Mol. Biol.* **1996**, *257*, 342–358.
- (140) Lichtarge, O.; Yamamoto, K. R.; Cohen, F. E. Identification of functional surfaces of the zinc binding domains of intracellular receptors. *J. Mol. Biol.* **1997**, *274*, 325–337.
- (141) Cerius² 4.7, Accelrys Inc., San Diego, CA.
- (142) Boehm, H. J. The computer program LUDI: A new method for the de novo design of enzyme inhibitors. *J. Comput. Aided Mol. Design.* **1992**, *6*, 61–72.
- (143) Boehm, H. J. LUDI: Rule based automatic design of new substituents for enzyme inhibitor leads. *J. Comput. Aided Mol. Design.* **1992**, *6*, 593–606.

JM049745W